Available online at sjuoz.uoz.edu.krd

journals.uoz.edu.krd

Science Journal of University of Zakho

Vol. 12, No.4 pp.450–455 October-December,2024

p-ISSN: 2663-628X
e-ISSN: 2663-6298

MORPHOLOGICAL AND OPTICAL PROPERTIES OF ZNO NANORODS GROWN ONTO SILICON SUBSTRATES: THE IMPACT OF GROWTH TEMPERATURE

Omar F. Farhat*[1], M. Husham [2], Azeez A. Barzinjy [2,3], Abbas M. Selmanan[4], A. A. Abuelsamen[5], Mohamed Bououdina[6], Asad A. Thahe[7]

[1]Physics Department, Faculty of Sciences, Alasmarya Islamic University, Zliten, Libya

[2]Department of Physics Education, Faculty of Education, Tishk International University (TIU), Erbil, KRG, Iraq

[3]Scientific Research center, Soran University, Kurdistan Region, Iraq

[4]Department of Pharmacognosy and Medicinal plants, Faculty of Pharmacy, University of Kufa, Najaf, Iraq

[5]Medical Imaging and Radiography Department, Aqaba University of Technology, Aqaba, Jordan

[6]Department of Mathematics and Sciences, Faculty of Humanities and Sciences, Prince Sultan University, Riyadh, Saudi Arabia

[7]Department of Medical Physics, College of applied science, University of Fallujah, Fallujah, Iraq

*Corresponding author: omarfarhat67@yahoo.com

Received: 1 Aug. 2024 / Accepted:15 Sep., 2024 / Published: 31 Oct., 2024. https://doi.org/10.25271/sjuoz.2024.12.3.1346

ABSTRACT

ZnO nanorods (NRs) have been successfully grown onto Silicon (Si) substrates. The properties of ZnO NRs have been characterized using field emission scanning microscopy, Photoluminescence, and X-ray diffraction. Results showed that the growth temperature (85, 90, 95, and 100ºC) significantly affected the properties of ZnO NRs. At a temperature of 95 ºC, the structural and optical properties have been significantly enhanced, besides, well-aligned ZnO NRs have been obtained. With the rise of growth temperature from 85 to 95ºC, the crystallite size increases (52 to 94 nm), and the near band edge emission to deep level emission ratio is enhanced. Besides, the aspect ratio for the prepared ZnO NRs has increased significantly reaching 19.42. This study emphasizes the significance of growth temperature in tunning the structural and microstructural and subsequently the physicochemical properties of ZnO NRs by fine control of the growth temperature. Moreover, a facile and cost-efficient method for fabricating ZnO nanorods for electronic applications based on silicon is presented in this study.

KEYWORDS: Growth temperature; optical properties; silicon substrates; structural, ZnO NRs.

1. INTRODUCTION

ZnO features a broad direct energy gap value between 3.37–3.80 eV with outstanding physical properties such as photoconductivity and transparency (Guo *et al.*, 2012). ZnO has garnered significant attention due to its exceptional properties, affordability, non-toxicity, and simplicity of production (Abdulrahman *et al.*, 2021). Nanostructured materials exhibit enhanced properties, including quantum confinement effects and a high surface-area-to-volume ratio, which surpass those of bulk materials (Guo *et al.*, 2012). The remarkable features of ZnO nanostructures make them ideal candidates for a range of environmental applications, including UV detection and gas sensing, and piezoelectric application. The high surface-to-volume ratio provided by nanostructures offers distinguished features for nanostructure-based devices. Various chemical and physical methods, including chemical bath deposition, have been utilized to grow different ZnO nanostructures (Farhat *et al.*, 2021), thermal oxidation (Farhat *et al.*, 2020), thermal evaporation (Bouhssira *et al.*, 2006) and chemical vapor deposition (Lee *et al.*, 2004). However, the growth temperature of ZnO nanostructures is of significant concern. Therefore, a moderate growth temperature is desirable due to factors such as the simplicity of the preparation and cost.

Researchers have focused on fabricating nanostructured materials on various substrates to adapt to both flexible and non-flexible devices (Altissimo *et al.*, 2010; Lim *et al.*, 2022; **S**herwan *et al.*, 2023). It has been highlighted that growth experimental parameters such as the growth temperature, duration, and precursor concentration significantly influence the properties of ZnO NRs (Farhat *et al.*, 2023; Husham *et al.*, 2015). Nonetheless, the impact of preparation temperature on ZnO NRs properties deposited on various substrates requires further investigation and optimization for prospective applications. Herein, the growth temperature has been varied within a narrow range (85 – 100ºC) and the evolution of structure (crystallinity), microstructure (diameter, length, and aspect ratio), and optical features of ZnO NRs prepared onto Si substrates, have been examined.

2. MATERIALS AND METHODS

For the preparation of ZnO NRs, the Si substrates were cleaned and prepared. The substrates cleaning process was explained elsewhere (Farhat *et al.*, 2017). Then, a ZnO seed layer was applied to the surface of the cleaned Si substrates by radio frequency (RF) sputtering. Sputtering was done under the flow of argon gas at a chamber pressure of 5.5 mTorr and sputtering power of 150 W. Then, the deposited seed layer was introduced to a furnace and annealed at 300 ºC. ZnO NRs grown using 0.05 M of zinc nitrate hexahydrate [Zn (NO_3) $6H_2O$] and hexamethylenetetramine (HTMA) ($C_6H_{12}N_4$). Precursors were separately dissolved in deionized water (DIW) in 100 ml beakers. After that, solutions were mixed and stirred at room temperature for 30 min. Si substrates were then immersed in the beaker vertically and heated by oven for 3h at various temperatures (80, 90, 95, and 100ºC). Finally, samples were removed from the beakers and rinsed with DIW. Morphological, optical, and structural properties of the grown NRs were characterized. The dimensions of vertically grown NRs were estimated using origin

* Corresponding author

software from the normal size distribution of NRs using ImageJ software.

3. RESULTS AND DISCUSSION

Morphological observations: FESEM analysis

Figure 1 shows the surface morphology properties of ZnO NRs grown onto Si substrates at different temperatures with the corresponding standard deviation measurements (STDV). As it can be seen, the NRs mean diameter varies as a function of the growth temperature. The average mean diameter for the prepared ZnO NRs is found to be 130, 128, 104, and 139 nm for NRs arrays grown at 85, 90, 95, and 100°C, respectively. Further, it is noticed that the ZnO NRs prepared at 85, 90, and 100°C bath temperatures revealed irregular size distribution. The average diameter varies between 60 – 200 nm. Conversely, NRs prepared at a temperature of 95°C exhibit a relatively uniform diameter distribution with the highest aspect ratio of 19.42. The size distribution of the prepared ZnO NRs can be attributed to variations in the rate of chemical reactions. The thermal degradation of HTMA releases hydroxyl ions into the solution through the reaction pathways. Subsequently, $Zn(OH)_2$ will be formed when Zn ions start to react with the hydroxyl ions as the hydroxyl ions reach supersaturation. Afterwards, $Zn(OH)_2$ decomposes to become ZnO. The formation of ZnO NRs can be explained by the chemical reactions represented by equations (1-4) (Zhang *et al.,* 2007):

$$(CH_2)_6N_4 + 6H_2O \rightarrow 6HCHO + 4NH_3 \quad (1)$$

$$NH_3 + H_2O \rightarrow NH_4^+ + OH^- \quad (2)$$

$$Zn^{2+} + 2OH^- \rightarrow ZnO\ (nuclei) + H_2O \quad (3)$$

$$Zn(OH)_4^{2-} \rightarrow ZnO + H_2O + 2OH^- \quad (4)$$

A temperature of 95 °C seems to be sufficient for the complete thermal decomposition of HMTA and $Zn(NO)_3$ to provide OH^- and Zn^{2+} ions, thereby enabling the formation of ZnO. This indicates that an adequate temperature enhanced the decomposition of HMTA resulting in the formation of ZnO NRs at relatively low temperatures with controlled diameter and length. It has been reported that, by adjusting the growth temperature, it is possible to enhance the development of ZnO NRs (Jaqsi *et al.,* 2023). Thus, high-density nanorods are formed because there are sufficient starting precursors. A small amount of Zn and OH ions lead to a slower nucleation rate, which induces a lower nanorod growth rate with enhanced properties.

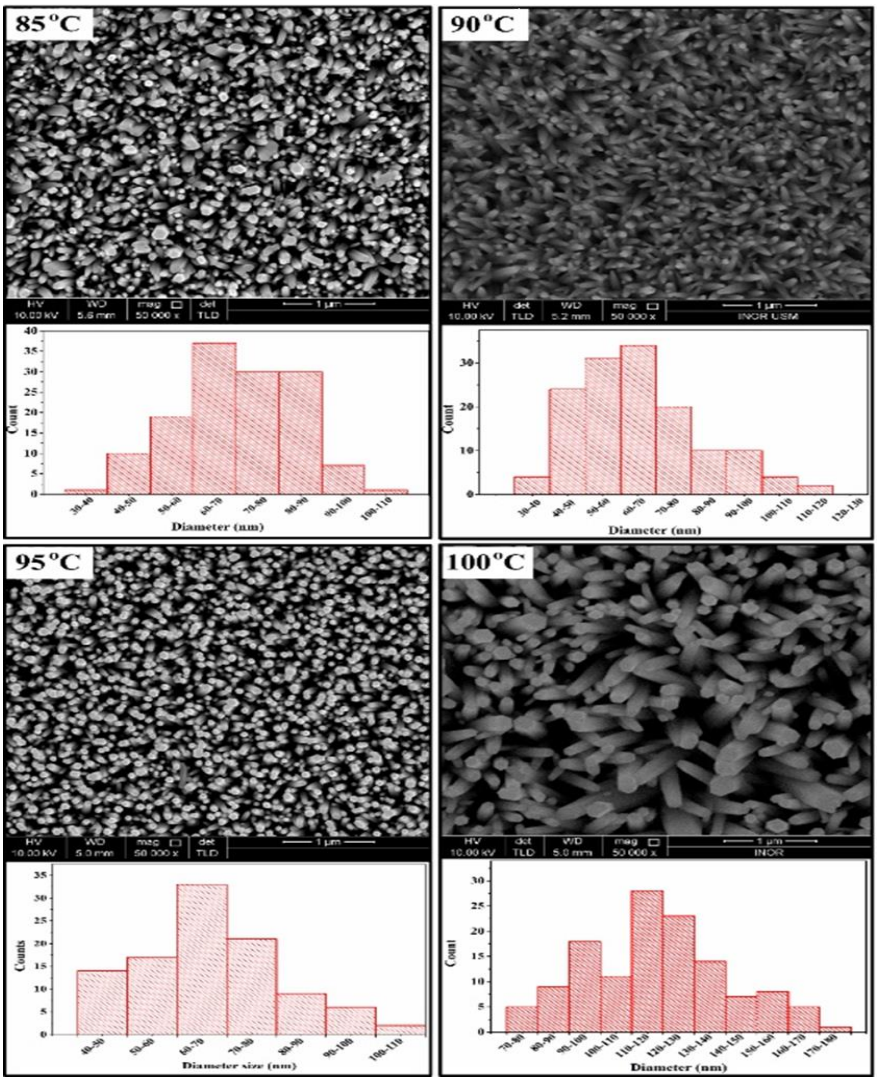

Figure 1: FESEM images with the corresponding STDV measurements of the grown ZnO NRs at different temperatures.

The HMTA has a crucial role in inhibiting the growth of the six crystalline planes of the NRs, which led to the development of ZnO NRs along the *c*-axis (Feng *et al.,* 2016). As the reaction temperature rises, the polar planes expand more rapidly, influencing the crystal's shape. As a result, higher Miller index planes with low surface energy are favored, encouraging the

growth of pencil-like ZnO nanorod arrays. Furthermore, the elevated surface mobility at higher temperatures causes the ZnO molecular species deposited on the base and surfaces to migrate to the tops of the nanorod arrays, ultimately producing a nanopencil-like structure as the ending product (Gu *et al.*, 2020). This manifests that the choice of an adequate temperature helps in enhancing the degradation of HMTA resulting in the formation of ZnO NRs along *c*-axis. Figure 2 depicts the FESEM cross-sectional view of ZnO NRs deposited onto Si substrate at different growth temperatures. As shown in the figure, well-aligned ZnO NR arrays with high density and uniform length have been successfully grown on the Si substrate surface, regardless of the growth temperature.

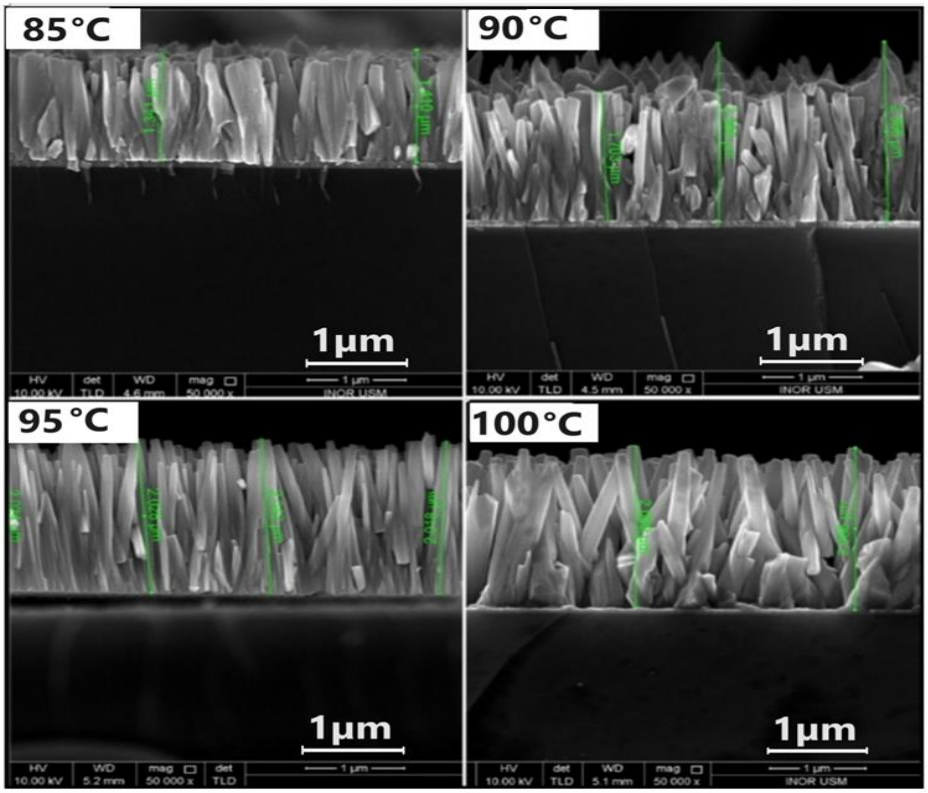

Figure 2: Cross-sectional for the grown ZnO NRs arrays p repared on Si substrate grown at different temperatures.

The estimated mean diameter, length, and aspect ratio of the grown NRs arrays are summarized in Table

Table 1: Variation of diameter, length, and aspect ratio with temperature of ZnO NRs.

Temperature (°C)	Diameter (nm)	length (nm)	Aspect ratio
85	130	1700	13.07
90	128	1431	11.18
95	104	2020	19.42
100	139	2100	15.10

Structural analysis: XRD characterization

Figure illustrates the XRD analysis of ZnO NRs grown onto Si substrates at different temperatures. Characteristic peaks corresponding to ZnO NRs and Si substrate, are observed. The prepared films a manifest pronounced diffraction peak at 2θ = 34.4° corresponding to the reflection (0 0 2) of the hexagonal lattice structure of ZnO phase, thus confirming that (002) is the preferred crystallographic orientation plane. The appeared peak at 2θ = 69.30° is assigned to the reflection (4 0 0) of the cubic lattice structure of the Si substrate, as referred in ICSD card No.01-080-0075. Interestingly, as the growth temperature increased from 85 to 100°C, diffracted peaks intensity is increased and become more defined. The dominant peak (0 0 2) intensity increases with increasing the chemical bath temperature, suggesting that the ZnO nanorods are vertically grown on the Si substrate surface with enhanced crystallinity.

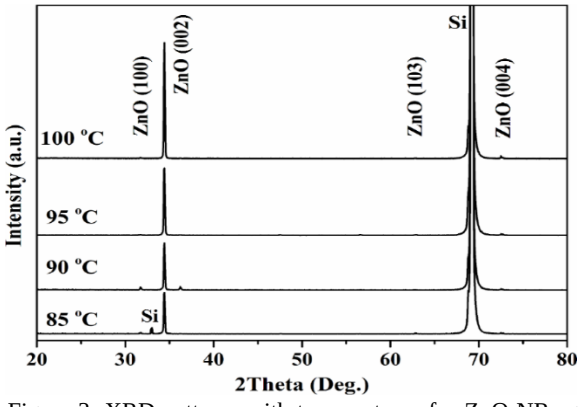

Figure 3: XRD patterns with temperatures for ZnO NRs grown on Si substrates.

Further, a slight peak shift for lower 2θ is noted, indicating that the as-grown ZnO nanorods exhibit residual compressive stress

caused by lattice parameter compression (Mosalagae *et al.*, 2020; Jaqsi *et al.*, 2023). This may be due to a mismatch between the lattice parameters of ZnO with a hexagonal lattice and Si with a cubic lattice.

Table 2 summarizes the structural (*d*-spacing and lattice parameter *c*) and microstructural (strain and crystallite size) parameters of ZnO NRs prepared at different temperatures. Lattice parameter (*c*) is calculated and compared with the unstrained lattice. It has been found that, the *c* value decreases with growth temperature as it was increased from 85 to 95°C, with a pronounced increase in crystallite size (from 37 to 57 nm). The minimal lattice compressive strain is found at 95°C. However, the compressive strain keeps increasing as the temperature rises to 100°C, accompanied by a notable decrease in crystallite size. This finding indicates that the crystallinity of the grown ZnO NRs is notably enhanced when the CBD temperature reaches 95ºC. Figures 4 a and b illustrate the lattice parameters and crystalline size for the prepared ZnO NRs as a function of the CBD temperature, respectively. As shown in Figure 4a, the lattice parameter of ZnO NRs gradually increases as the growth temperature rises from 85°C to 95°C, but then unexpectedly decreases beyond 95°C. The obtained lattice parameter results of ZnO NRs are in good agreement with (Ahmed *et al.*, 2021). The crystallite size (*D*) of the synthesized ZnO NRs follows a trend similar to that of the lattice parameters. The crystallite increased as the growth temperatures rose from 85°C to 95°C, indicating an enhancement in crystal quality, as shown in Figure 4b.

Table 2 presents the structural analyses of the grown ZnO NRs. The table shows that, the highest lattice parameter value was attained at a growth temperature of 95°C. Besides, ZnO NRs grown at 95°C possess the lowest compressive strain. However, when the growth temperature increased to 100°C, the compressive strain increased further, while the crystallite size decreased to 54 nm. Thus, based on this assertion, the crystallinity of ZnO NRs is significantly improved when the CBD temperature reaches 95°C.

Table 2: Structural analyses of ZnO NRs grown on Si substrates with different temperatures

Temperature (°C)	**2θ (°)**	**d (Å)**	**FWHM (°)**	**c (Å)**	**ε_z (%)**	**D (nm)**
Unstrained				5.2098		
85	34.43	2.6028	0.2311	5.2056	-0.0806	37
90	34.42	2.6030	0.2101	5.2060	-0.0729	41
95	34.41	2.6039	0.1519	5.2078	-0.0383	57
100	34.42	2.6029	0.1583	5.2058	-0.0767	54

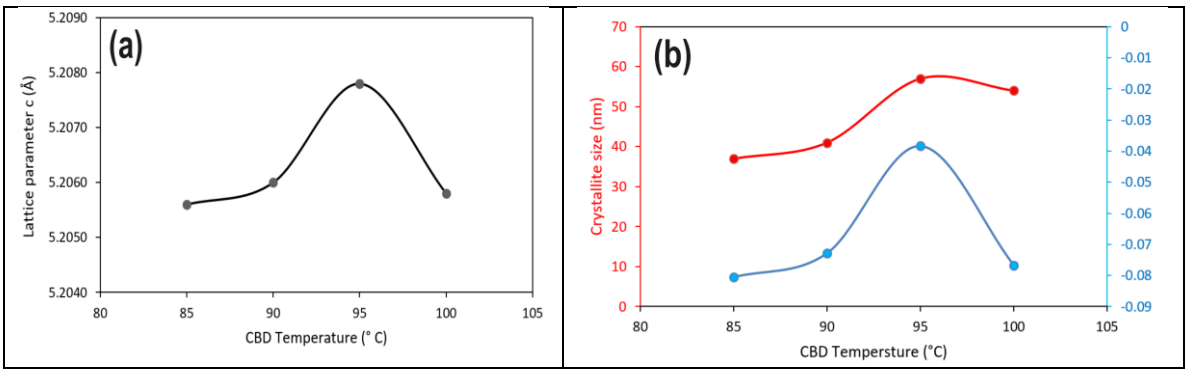

Figure 4: Evolution of (a) lattice parameter and (b) Strain and crystallite size as function of CBD temperature.

Optical properties : Photoluminescence (PL) analysis Error! Reference source not found.5 demonstrates the PL m easurements for ZnO NRs grown onto Si substrates at different temperatures.

As can be seen, all PL spectra manifest two peaks corresponding to ZnO emission bands. The dominant peak was observed to be located at about 378 nm which was attributed to the near-band edge (NBE) emission of ZnO energy gap. This emission is because of the recombination of free excitons (Wang, 2012). The broad peak observed in the 460–700 nm range (visible region) is attributed to the deep-level emissions (DLE) of ZnO. Interestingly, the latter is the most detected emission in ZnO nanostructures. It is ascribed to the structural defects in ZnO crystals such as oxygen vacancy, zinc vacancies, and other associated structural defects (Hu *et al.*, 2010). When UV light illuminates ZnO NRs, vacancies become prone to the holes generated upon the exposure of UV. Therefore, photons could be emitted in the visible region due to the electron-hole recombination at the oxygen vacancies (Selman *et al.*, 2014). Further, no considerable shift is observed in the NBE peak position with the increase of the crystallite size due to grain growth accompanying the rise of CBD temperature. However, a slight red shift was detected for the film prepared at 100 ºC. Notably, peaks' intensity is found to enhance as the temperature increased from 85 to 100ºC. This agrees with the XRD analysis, where the crystallinity is enhanced, and the crystallite size increases as the temperature in the CBD rises.

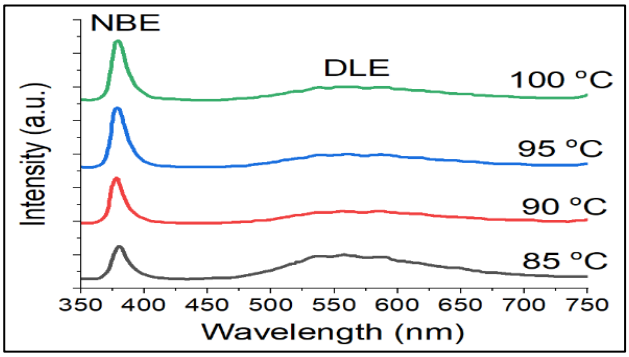

Figure 5: PL spectra as a faction of temperature for ZnO NRs grown on Si substrates

Table 3 summarizes the optical analyses for ZnO NRs grown at different temperatures.

Table 3: PL spectra for the prepared ZnO NRs on Si substrates at different temperatures.

Temperature (ºC)	NBE Position (nm)	Band gap (eV)	FWHM (nm)	(NBE/DLE) Ratio
85	381.13	3.25	17.93	0.970
90	379.80	3.26	13.77	1.772
95	379.80	3.26	13.94	2.521
100	381.64	3.25	15.66	2.293

As shown in Table 3, the NBE/DLE ratio increased as the growth temperature increased and attained a maximum value of 95ºC. The increase in NBE/DLE ratio indicates that the ZnO NR structure possessed a high-crystal quality with minimum structural defects (Fan *et al.*, 2010; Husham *et al.*, 2015). The enhancement of nanostructure optical characteristics can be attributed to the high intensity of the UV emission peak combined with a minimal density of defect in the PL spectra (Hassan *et al.*, 2012).

4. CONCLUSIONS

ZnO NRs were successfully grown onto Si substrates by a simple cost-effective CBD technique with fine tuning of bath temperature. XRD measurements showed a well crystalline ZnO NRs. Structural and microstructural parameters were found sensitive to the CBD temperature. Besides, surface morphology analyses for the grown ZnO NRs showed well aligned ZnO NRs grown perpendicularly to the substrates. Results showed that the optical and structural properties remarkably improved with the rise of the growth temperature. At a growth temperature of 95°C, the crystallite size, the aspect ratio, and the strain reached the optimum values, consequently leading to enhanced optical properties. Indeed, the ratio of NBE/DLE improved as revealed by PL analysis. Analyses showed that the properties of ZnO NRs can be modified by a fine control of preparation temperature. Additionally, the report presented a simple method to prepare high crystalline ZnO NRs grown on Si substrates for important silicon-based applications.

ACKNOWLEDGMENTS

The authors sincerely appreciate the support from Universiti Sains Malaysia (USM) for their assistance this work under Grant number 304/PFIZIK/6313095. The author would like to thank Prince Sultan University for their support.

REFERENCES

Ahmed F.A., Sabah M. A., Azeez A. B., Samir M. H., Naser M. A., Munirah A. A. **(**2021). Fabrication and Characterization of High-Quality UV Photodetectors Based ZnO Nanorods Using Traditional and Modified Chemical Bath Deposition Methods. Nanomaterials 11, 677. https://doi.org/10.3390/nano11030677

Altissimo, M. (2010). E-Beam lithography for micro-/nanofabrication. Bio microfluidics, 4, 026503. https://doi.org/10.1063/1.3437589

Bouhssira N., Abed S., Tomasella E., Cellier J., Mosbah A., Aida M. S., & Jacquet M. (2006). Influence of annealing temperature on the properties of ZnO thin films deposited by thermal evaporation. Applied Surface Science, 252, 5594-5597.https://doi.org/10.1016/j.egypro.2012.07.008

Fan D., Zhang R., & Wang X. (2010). Synthesis and ultraviolet emission of aligned ZnO rod-on-rod nanostructures. Solid state communications, 150, 824-827. https://doi.org/10.1016/j.ssc.2010.02.013

Farhat O. F., Husham M., Bououdina M., Abuelsamen A. A., Oglat A. A., & Mohammed N. J. (2021). Tape-based novel ZnO nanoaggregates photodetector. Sensors and Actuators A: Physical, 332, 113210. https://doi.org/10.1016/j.sna.2021.113210

Farhat O. F., Hisham M., Bououdina M., Oglat A. A., & Mohammed N. J. (2020). Growth of ZnO nanostructures by wet oxidation of Zn thin film deposited on heat-resistant flexible substrates at low temperature. Semiconductors, 54, 1220-1223. https://doi.org/10.1134/S1063782620100103

Farhat O. F., Husham M., ALDelfi H. H., & Bououdina M. (2023). Tuning the diameter and optical properties of ZnO nanorods grown onto flexible substrates at different temperatures. Journal of Crystal Growth, 607, 127115. https://doi.org/10.1016/j.jcrysgro.2023.127115

Farhat O. F., Halim M. M., Ahmed N. M., Oglat A. A., Abuelsamen A. A., Bououdina M., & Qaeed M. A. (2017). A study of the effects of aligned vertically growth time on ZnO nanorods deposited for the first time on Teflon substrate. Applied Surface Science, 426, 906-912. https://doi.org/10.1016/j.apsusc.2017.07.031

Feng W., Wang B., Huang P., Wang X., Yu J., & Wang C. (2016). Wet chemistry synthesis of ZnO crystals with hexamethylenetetramine (HMTA): Understanding the role of HMTA in the formation of ZnO crystals. Materials Science in Semiconductor Processing, 41, 462-469. https://doi.org/10.1016/j.mssp.2015.10.017

Gu P., Zhu X., & Yang D. (2020). Vertically aligned ZnO nanorods arrays grown by chemical bath deposition for ultraviolet photodetectors with high response performance. Journal of Alloys and Compounds, 815, 152346. https://doi.org/10.1016/j.jallcom.2019.152346

Guo L., Zhang H., Zhao D., Li B., Zhang Z., Jiang M., & Shen D. (2012). High responsivity ZnO nanowires-based UV detector fabricated by the dielectrophoresis method. Sensors and Actuators B: Chemical, 166, 12-16. https://doi.org/10.1016/j.snb.2011.08.049

Hu A., Wu F., Liu J., Jiang J., Ding R., Li X. & Huang X. (2010). Density-and adhesion-controlled ZnO nanorod arrays on the ITO flexible substrates and their electrochromic performance. Journal of Alloys and Compounds, 507, 261-266. https://doi.org/10.1016/j.jallcom.2010.07.173

Hassan J.J., Mahdi M. A., Kasim,S. J., Ahmed N. M., Abu Hassan H., & Hassan Z. (2012). High sensitivity and fast response and recovery times in a ZnO nanorod array/p-Si self-powered ultraviolet detector. *Applied Physics Letters*, *101*(26). https://doi.org/10.1063/1.4773245

Husham M., & Hassan Z. (2015). Synthesis of nanocrystalline CdS thin films via microwave-assisted chemical bath deposition for highly photosensitive and rapid response photodetectors. Journal of Nanoelectronics and Optoelectronics,10,783-789. https://doi.org/10.1016/j.sna.2015.04.010

Husham M., Hassan Z., Selman A.M., Allam N.K. (2015). Microwave-assisted chemical bath deposition of nanocrystalline CdS thin films with superior photodetection characteristics, Sensors and Actuators A 230, 9–16. https://doi.org/10.1016/j.sna.2015.04.010

Jaqsi M.K., Kareem A., & Abdullrahman A. (2023). Investigating the impact of growth temperatures on the ZnO nanorods properties grown with simplest spray technique. Scientific journal of the University of Zakho, 11,112–118. https://doi.org/10.25271/sjuoz.2023.11.1.1072

Lim Y.H., Choi H-J, & Lee J. (2022). Fabrication of nanostructures on a large-area substrate with a minimized stitch error using the step-and-repeat nanoimprint process.Materials, 15,6036. https://doi.org/10.3390/ma15176036

Mosalagae K., Murape D. M., & Lepodise L. M. (2020). Effects of growth conditions on properties of CBD synthesized ZnO nanorods grown on ultrasonic spray pyrolysis deposited ZnO seed layers. Heliyon, 6, e04458. https://doi.org/10.1016/j.heliyon.2020.e04458

Mohammed H. K., Raghad Y. M., Mohammed A. I. (2023). Influence of annealing temperature on Zinc Oxysulfide thin films properties deposited by thermal spray technique. Scientific journal of the University of Zakho, 11,600-605. https://doi.org/10.25271/sjuoz.2023.11.4.1192

Selman A. M., Hassan Z., & Husham M. (2014). Structural and photoluminescence studies of rutile TiO_2 nanorods prepared by chemical bath deposition method on Si substrates at different pH values. Measurement, 56, 155-162. https://doi.org/10.1016/j.measurement.2014.06.027

Sherwan M.I., Sabah M.A. (2023). The effect of calcination temperature on the properties of ZnO Nanoparticles synthesized by using leaves extacts of Pinus Brutia tree. Scientific journal of the University of Zakho, 11, 286–297. https://doi.org/10.25271/sjuoz.2023.11.2.1087

Woong L., Jeong M. C., & Myoung J. M. (2004). Catalyst-free growth of ZnO nanowires by metal-organic chemical vapour deposition (MOCVD) and thermal evaporation. Acta Materialia, 52, 3949-3957. https://doi.org/10.1016/j.actamat.2004.05.010

Zhang Z., Wang S. J., Yu T., & Wu T. (2007). Controlling the growth mechanism of ZnO nanowires by selecting catalysts. The Journal of Physical Chemistry C, 111, 17500-17505. https://pubs.acs.org/doi/10.1021/jp075296a